

RESEARCH PAPER



# The stress-activated protein kinase pathway and the expression of stanniocalcin-1 are regulated by miR-146b-5p in papillary thyroid carcinogenesis

Abeer Al-Abdallah <sup>a</sup>, Iman Jahanbani<sup>a</sup>, Heba Mehdawi<sup>a</sup>, Rola H Ali<sup>a</sup>, Nabeel Al-Brahim<sup>b</sup>, and Olusegun Mojiminiyi<sup>a</sup>

<sup>a</sup>Pathology Department, Kuwait University, Kuwait City, Kuwait; <sup>b</sup>Pathology Department, Farwaniya Hospital, Kuwait City, Kuwait

## ABSTRACT

Papillary thyroid cancer (PTC) is the most common type of thyroid cancer. Deciphering the pathophysiological mechanisms that contribute to PTC development is essential to the discovery of optimal diagnostic and therapeutic approaches. MiR-146b-5p has been identified as a cancer-associated microRNA highly up-regulated in PTC. This study explores the hypothesis that miR-146b-5p contributes to papillary thyroid carcinogenesis through regulation of cell signaling pathways in a manner that overcomes the cellular growth suppressive events and provides survival advantage. The effect of miR-146b-5p inhibition on major cancer related signaling pathways and expression of Stanniocalcin-1 (STC1), an emerging molecule associated with stress response and carcinogenesis, was tested in cultured primary thyroid cells using luciferase reporter assays, quantitative real-time PCR, immunofluorescence staining, and flow cytometry. Our results demonstrated that miR-146b-5p inhibits the JNK/AP1 pathway activity and down-regulates the expression of STC-1 in thyroid-cultured cells and in thyroid tissue samples. In the presence of miR-146b-5p, PTC cells were resistant to cell death in response to oxidative stress. This is a novel report that miR-146b-5p directly targets STC1 and regulates the activity of JNK/AP1 pathway. Considering the importance of the JNK/AP1 pathway and STC1 in mediating many physiological and pathological processes like apoptosis, stress response and cellular metabolism, a biological regulator of these pathways would have a great scientific and clinical significance.

## ARTICLE HISTORY

Received 27 February 2019  
Revised 31 October 2019  
Accepted 20 January 2020

## KEYWORDS

miRNA, papillary thyroid carcinoma; stanniocalcin-1; stress-activated protein kinase; activator protein-1

## Introduction

The incidence of thyroid cancer has been increasing worldwide, largely driven by the increase in papillary thyroid cancer (PTC).<sup>1,2</sup> Etiology and risk factors identification as well as proper clinical management, all depend on our understanding of the pathophysiological mechanisms contributing to the initiation and progression of PTC. Multiple genes and cellular pathways have been reported to participate in the occurrence and development of thyroid cancer.<sup>3–5</sup> MicroRNAs (miRNAs) have emerged in the last decade as promising molecular markers due to their distinct expression in different types of cancer including thyroid cancer.<sup>6–9</sup> Through their function in blocking the translation or degrading the target mRNAs, they are expected to play important roles in thyroid cancer biogenesis and progression.<sup>10–12</sup>

MiR-146b-5p has been identified as a cancer-associated miRNA with oncogenic and tumor-suppressive activity.<sup>13–16</sup> These contrasting roles may be explained by the differences of the targets regulated by miR-146b-5p in different tissues. In PTC, miR-146b-5p has been reported to be up-regulated and associated with aggressive tumor behavior.<sup>17,18</sup> However, only a small number of published studies explored the functional targets of miR-146b-5p and its role in PTC.<sup>13,19–22</sup> Our previous study showed that miR-146b-5p is highly up-regulated in classic PTC (cPTC).<sup>23</sup> The purpose of this study is to identify the mechanisms by which miR-146b-5p regulates the molecular events supporting papillary thyroid carcinogenesis.

In the course of investigating the role of miR-146b-5p in PTC, we found that Stanniocalcin-1 (STC1) is a target of miR-146b-5p. STC1 is a highly conserved glycoprotein that has a physiologic role in regulating serum calcium and phosphate in fish and rats.<sup>24,25</sup> A number of studies suggested multiple roles for mammalian STC1 in angiogenesis,<sup>26</sup> inflammation,<sup>27</sup> cellular metabolism,<sup>28</sup> and cancer.<sup>29,30</sup> Additional studies demonstrated that STC1 is involved in the cellular stress response; STC1 expression was shown to be up-regulated in response to hypoxia<sup>31</sup> and oxidative stress.<sup>32</sup> Furthermore, STC1 is regulated by the tumor suppressors BRCA1<sup>33</sup> and p53,<sup>34</sup> both of which play key roles in orchestrating DNA repair, growth arrest and apoptosis, in response to various cellular stresses. There are few publications on the expression of STC1 in papillary thyroid cancer<sup>35</sup> and no previous publications on its regulation. We demonstrate here that miR-146b-5p regulates the expression of STC1 and the activation of the stress kinase JNK/AP1 pathway in PTC.

## Results

### *MiR-146b-5p reduces the MAPK/JNK/AP1 signaling pathway activity*

In order to understand the functional impact of miR-146b-5p up-regulation in PTC, we investigated the effect of inhibiting the expression of miR-146b-5p on signal transduction pathways relevant to carcinogenesis, using miR-146b-5p inhibitor and luciferase

reporter assays. First, we have established primary cultures of thyroid cells obtained from fresh thyroid tumor samples. Cultured cells were used from first passage and their identity as epithelial thyroid cells were confirmed by immunostaining with cytokeratin and thyroglobulin specific antibodies (Figure 1). MiR-146b-5p inhibitor was transfected into the cultured thyroid cells as described in the Methods section. MiR-146-5p expression level was determined in the transfected and control cells to confirm successful inhibition (Table 1). MiR-146-5p inhibition increased significantly the relative luciferase activity of the MAPK/JNK/AP1 pathway in PTC samples with high miR-146b-5p endogenous level (Samples 1, 2 and 3;  $p$ -value = 0.02). Inhibition of miR-146b-5p had only minimal effect in samples with low endogenous miR-146b-5p level (Samples 4 to 8) and insignificant effect on the other pathways tested (Table 1). We also analyzed the endogenous MAPK/JNK/AP1 activity in different samples in relation to the endogenous miR-146b-5p expression level; The samples were all transfected with the pathway reporters constructs with no miR-146b-5p inhibitor. The JNK pathway reporter activity in the PTC samples was compared to the JNK activity in the MNG samples used as controls. The calculated fold change was then correlated with the miR-146b-5p expression level in these samples. We found that in PTC, the endogenous MAPK/JNK/AP1 pathway activity is inversely correlated with the expression of miR-146b-5p ( $R = -0.91$ ) (Figure 2). Altogether these results demonstrate that miR-146b-5p has an inhibitory effect on the MAPK/JNK/AP1 pathway.

### **The JNK/AP1 pathway is activated after mir-146b-5p inhibition in PTC cultured cells**

MiR-146b-5p inhibitor was labeled with fluorescein dye before transfection as explained in the Methods section. Immunofluorescence staining with AP1 specific antibody showed that nuclear AP1 appeared specifically in the cells that have taken the labeled miR-146b-5p inhibitor; Treatment with miR-146b-5p inhibitor caused AP1 to appear in the nuclei of thyroid epithelial cells (cytokeratin positive cells) (Figure 3). Immunofluorescence stain and immunoblot experiments showed that  $p$ -JNK is expressed in PTC cells transfected with miR-146b-5p inhibitor while it is not expressed in the cells transfected with negative control (Figure 4a,b). No clear effect of miR-146b-5p inhibition on the expression of  $p$ -ERK,  $p$ -p38, and NF $\kappa$ B was observed (Figure S-1). These findings demonstrate that miR-146b-5p inhibition results in the activation of the JNK/AP1 pathway in cultured thyroid follicular cells.

### **JNK pathway activation and miR-146b-5p up-regulation show a mutually exclusive relation in thyroid tissues**

We tested the activation status of the JNK pathway in FFPE tissue samples from 30 cPTC, 10 NIFTP, and 10 MNG cases (Diagnostic histopathological classification is explained in the Materials and Methods section 1), by immunofluorescence

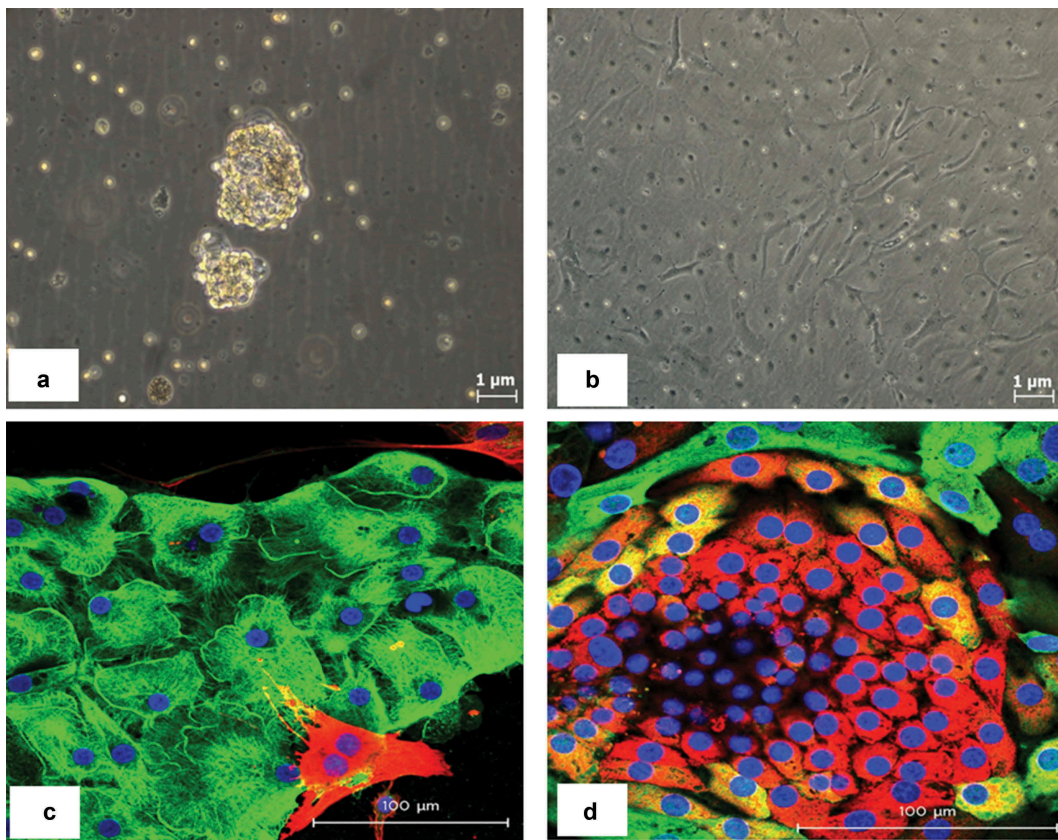


**Figure 1.** Primary thyroid cancer cells culture and characterization. (a) Thyroid cells forming follicles in the first week of culture. (b)- Thyroid cells confluent growth. (c) Immunofluorescence staining with the epithelial marker, cytokeratin (green) and the mesenchymal marker, smooth muscle actin (red). (d) Immunofluorescence staining with  $p$ -ERK (green) and thyroglobulin (red) confirming that the cultured cells are thyroid follicular cells. Blue stain is the DAPI nuclear stain.

**Table 1.** Changes in signaling pathways activities in thyroid cancer cells in response to miR-146b-5p inhibition.

Sample (Diagnosis)	miR-146b-5p expression level <sup>a</sup>		Pathway (Transcription factor) activity <sup>b</sup>				
	-/miR-146b-5p inhibitor	+/miR-146b-5p inhibitor	p53	NFκB	Hypoxia	MAPK/ERK	MAPK/JNK
			p53	NFκB	HIF1A	Elk-1/SRF	AP-1
1 (PTC)	10.76	-7.82	1.85	-1.10	-1.57	-1.02	4.14
2 (PTC)	15.99	-47.72	1.24	-6.76	1.50	-1.00	8.98
3 (PTC)	29.05	-43.07	1.41	-1.12	-1.06	-1.32	12.07
<b>p-value <sup>c</sup></b>		<b>&lt;0.001</b>	<b>0.10</b>	<b>0.08</b>	<b>0.28</b>	<b>0.17</b>	<b>0.02</b>
4 (PTC)	2.12	-5.85	1.10	-1.53	-3.21	-1.26	1.01
5 (PTC)	1.60	-0.63	1.67	-1.67	1.35	1.46	1.92
6 (PTC)	3.78	-1.27	1.69	-1.78	-2.94	-1.61	1.71
7 (PTC)	1.09	-50.00	2.04	-1.39	-1.46	-1.33	1.06
8 (MNG)	-1.28	-1.07	1.56	1.27	1.23	-1.11	1.43
<b>p-value <sup>d</sup></b>		<b>&lt;0.001</b>	<b>0.03</b>	<b>0.45</b>	<b>0.47</b>	<b>0.07</b>	<b>0.14</b>

a: miR-146b-5p level expressed as fold change compared to MNG controls; b: Pathway activity expressed as fold change of the luciferase activity of cells transfected with miR-146b-5p inhibitor compared to cells transfected with negative control. c: Statistical analysis of the pathways' activities of samples with high miR146b-5p level (Samples # 1 to 3) using paired samples Student's *t*-test. d: Statistical analysis of the pathways' activities of samples with low miR146b-5p level (Samples # 4 to 8) using paired samples Student's *t*-test.

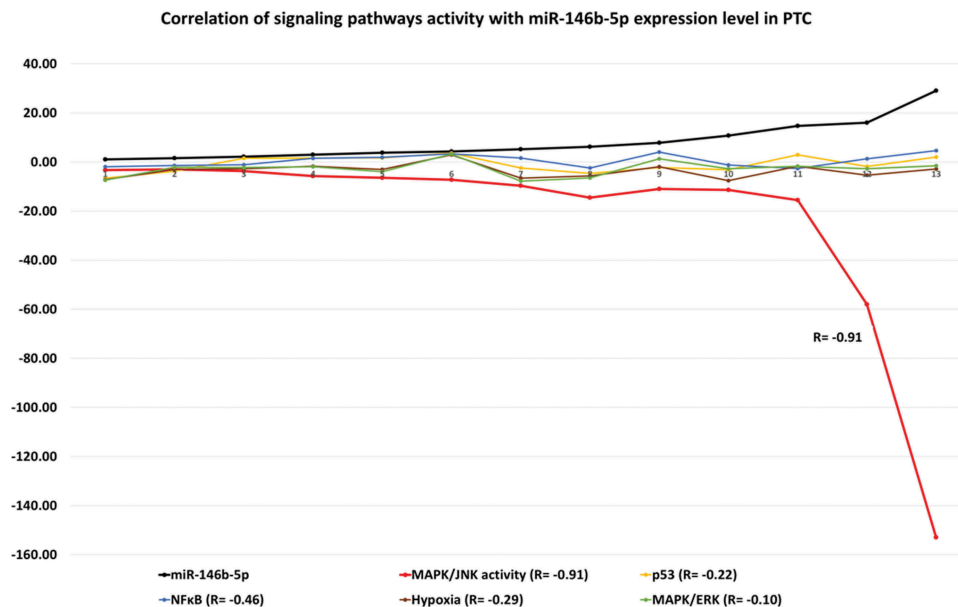


**Figure 2.** Cell signaling pathways endogenous activity in PTCs in relation to miR-146b-5p expression level. The activity of each signaling pathway is calculated by comparing the normalized luciferase activity in transfected experimental samples (PTC, *n* = 13) versus control (MNG, *n* = 3) all without miR-146b-5p inhibitor. Fold Change = (firefly/renilla ratio of PTC)/(firefly/renilla ratio of MNG). Samples in the Luciferase assays were run in quadruplicates. JNK/AP1 is the only pathway that showed a significant inverse correlation with the level of miR-146b-5p expression (*R* = -0.91).

staining with *p*-JNK specific antibody. Cases were considered positive if non-ambiguous cytoplasmic and/or nuclear staining was identified in the thyroid follicular tumor cells only. It was noted that some immune cells infiltrating the tumor are in some cases positive for *p*-JNK; The presence of these cells was not considered as positivity. Representative pictures of the different histopathological types tested are shown in Figure 5. Nuclear *p*-JNK was observed in 8/10 (80%) of NIFTP, 7/10 (70%) of MNG, and 7/30 (23%) of cPTC cases. In 23/30 (77%) of cPTC samples, no *p*-JNK could be detected in the tumor cells. Correlating the *p*-JNK status with the level of miR-146b-5p expression, our results showed that PTCs with positive *p*-JNK express significantly lower levels of miR-146b-5p than PTCs with negative *p*-JNK (*P* = .0001) (Figure 5b). It should be noted here that samples of NIFTP and MNG which showed positive expression of -JNK in most

of the cases, also expressed a low level of miR-146b-5p as estimated by real-time PCR (Table 2).

### **Mir-146b-5p negatively regulates cell death in response to oxidative stress**

Cultured PTC cells transfected with miR-146b-5p inhibitor were tested in apoptosis assay by flow cytometry. MiR-146b-5p inhibition without exposure to oxidative stress did not affect PTC cell death ability. However, inhibition of miR-146b-5p along with exposure of cultured cancer cells to oxidative stress resulted in increased percentage of dead cells (Figure 6). These results indicate a negative regulatory effect of miR-146b-5p on cell death events in response to oxidative stress in PTC.

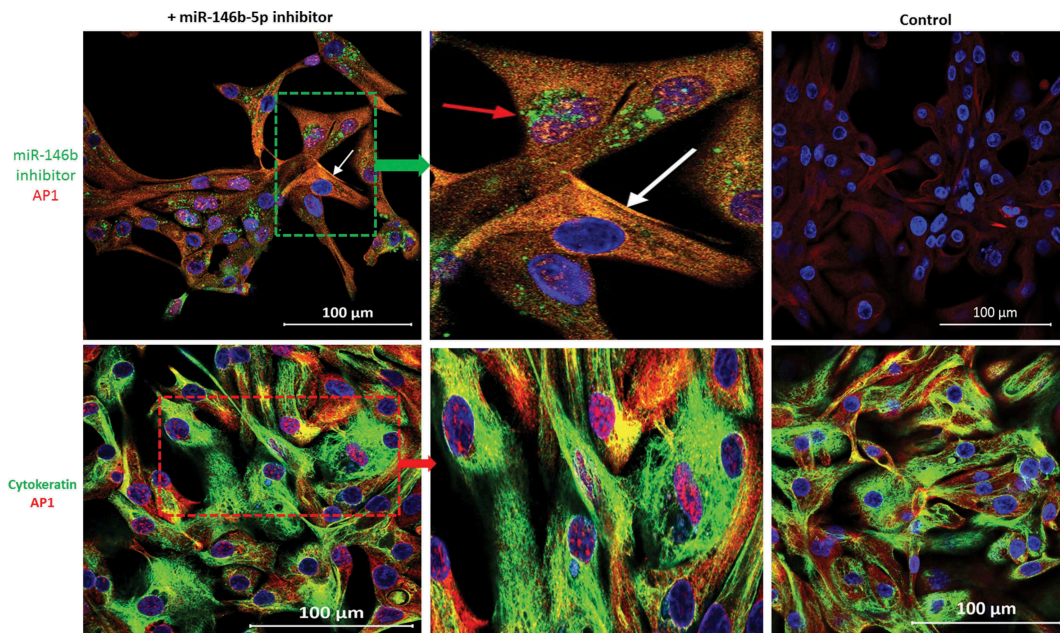


**Figure 3.** Immunofluorescence staining showing qualitatively the effect of miR-146b-5p inhibition on AP1 expression in a representative transfected PTC sample. (a) Representative image showing that the presence of miR-146b-5p inhibitor (green fluorescence) is accompanied by nuclear expression of AP1 (red arrow); in the same field the absence of the inhibitor (cell indicated by white arrow) has no nuclear AP1. (b) Representative image showing nuclear expression of AP1 (red fluorescence) in the thyroid epithelial cells (cytokeratin positive – green fluorescence) treated with miR-146b inhibitor, while no nuclear AP1 is detected in the cells transfected with negative control. Blue stain is the DAPI nuclear stain.

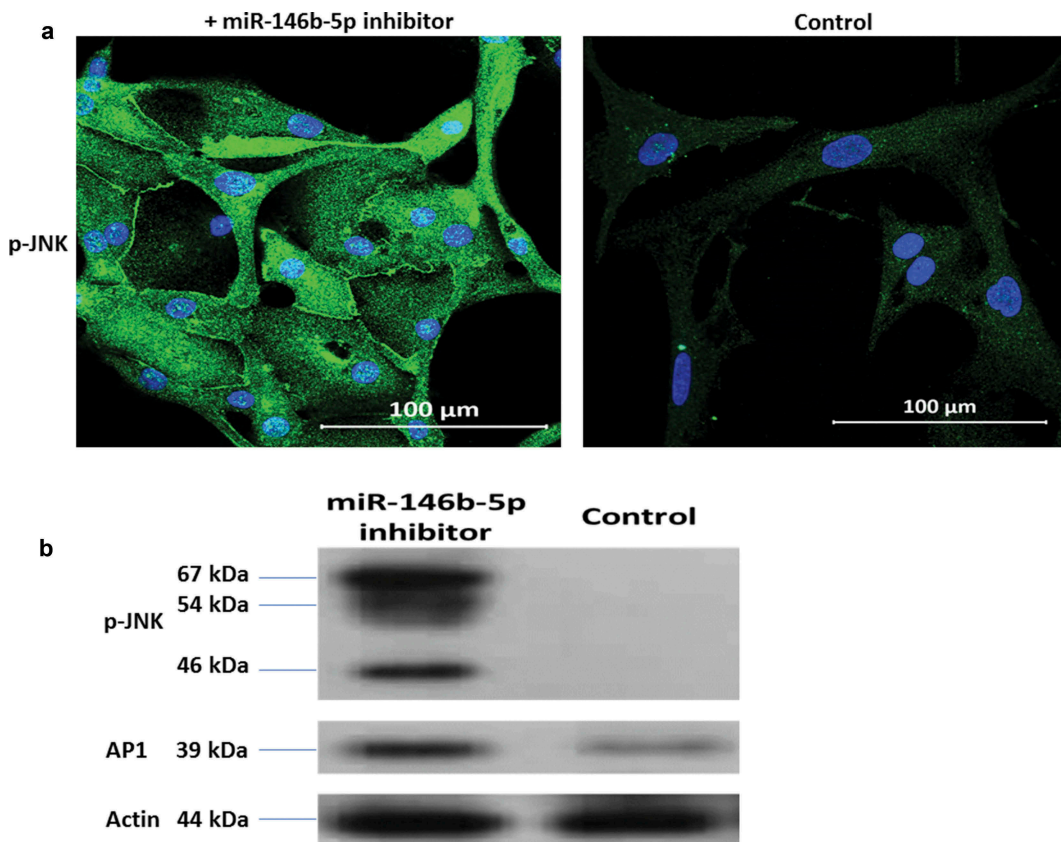


**Figure 4.** Effect of miR-146b-5p inhibition on the expression of phospho-JNK. (a) Nuclear/cytoplasmic *p*-JNK (Green) is detected in thyroid cells transfected with miR-146b-5p inhibitor while control cells are negative. (b) Immunoblot showing protein expression of *p*-JNK (three isoforms of 46, 54 and 67 kDa) and AP1 (39 kDa) in thyroid cells transfected with miR-146b-5p inhibitor with less or no expression in cells transfected with negative control.

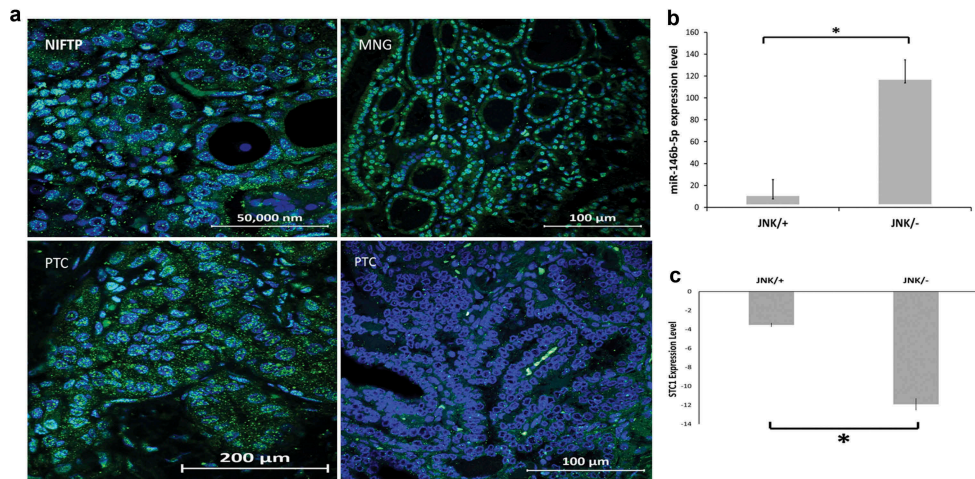


**Figure 5.** Expression and localization of *p*-JNK in different thyroid lesions. (a) Immunofluorescence staining of *p*-JNK (green) is detected in the nuclei of thyroid follicular cells in NIFTP and in MNG. PTC show positive nuclear *p*-JNK stain in some cases (picture at the lower left) and negative staining in most of the cases (picture at lower right). Nuclei are stained blue with DAPI. (b) Bar graph showing that the PTC group with negative *p*-JNK express a significantly higher level of miR-146b-5p when compared to the group with positive *p*-JNK ( $P = .0001$ ). (c) Bar graph showing that STC1 expression is significantly more downregulated in the PTC group with negative *p*-JNK compared to the group with positive *p*-JNK ( $P = .01$ ).

**Table 2.** Expression of STC1 and miR-146b-5p in thyroid tissues.

	Mean expression value ( $\Delta$ Ct $\pm$ SD)			PTC vs. MNG		PTC vs. NIFTP	
	MNG ( $n = 10$ )	NIFTP ( $n = 10$ )	PTC <sup>§</sup> ( $n = 20$ )	Fold change	$p$ -value*	Fold change	$p$ -value*
STC1	$0.42 \pm 1.15$	$0.53 \pm 0.52$	$2.51 \pm 1.38$	-4.27	0.0003	-3.95	0.0001
miR-146b-5p	$3.78 \pm 1.06$	$3.01 \pm 2.87$	$-0.68 \pm 0.47$	22.03	<0.0001	12.92	0.0003

§ PTC samples used here are all JNK negative as proved by immunostaining results. \*Statistical analysis was done using Student's *t*-test.

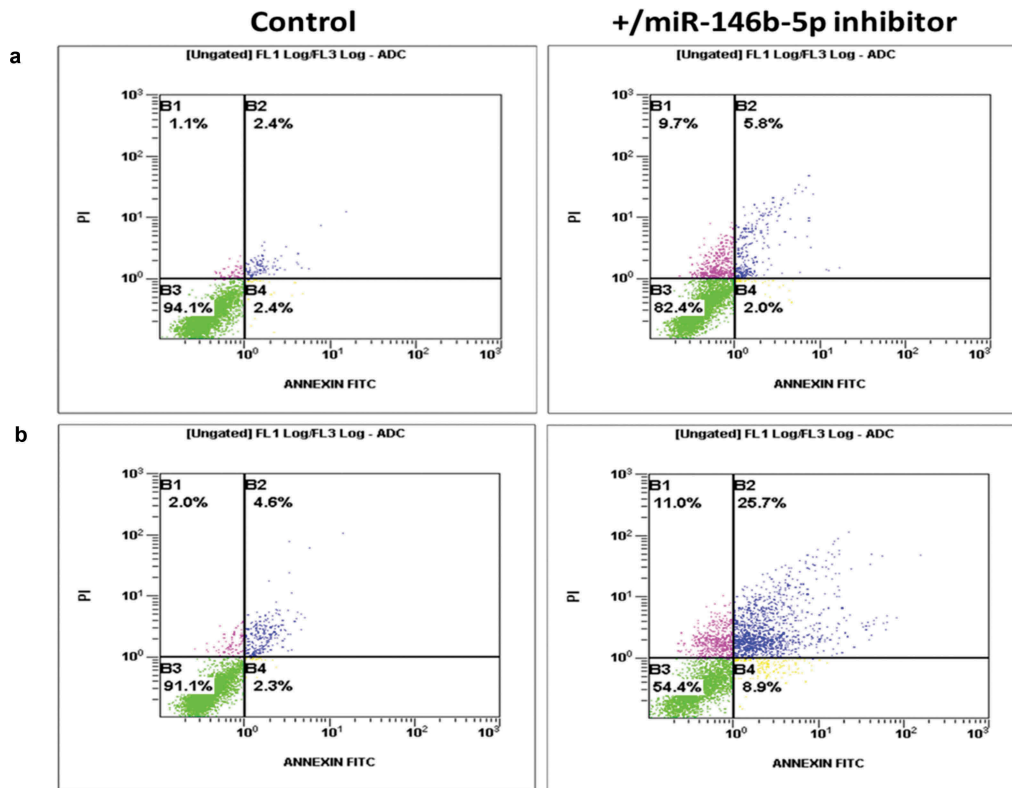


**Figure 6.** miR-146b-5p protects PTC cells from cell death in response to oxidative stress (Representative of three independent experiments). (a) Primary thyroid cancer cells transfected with miR-146b inhibitor showed minimal increased number of dying cells (quadrants B1, B2 and B4; 18%) compared to cells transfected with negative control (6%). (b) Under oxidative stress conditions, cells transfected with miR-146b inhibitor showed increased number of dying cells (quadrants B1, B2 and B4; 46%) compared to cells transfected with negative control (9%). Comparing A to B, these results show that in the presence of high endogenous level of miR-146b-5p, PTC cells are resistant to cell death when exposed to oxidative stress (no significant difference between stress (9%) and no stress (6%) conditions).

**Table 3.** Effect of miR-146b-5p inhibition on the expression of STC1 gene in thyroid cancer cells.

Samples	STC1 expression – ΔCt (SD)		Fold Change	p-value*
	Control	+miR-146b-5p inhibitor		
1	1.60 (0.36)	-0.93 (1.02)	5.78	0.0003
2	1.29 (0.49)	-0.56 (1.04)	3.61	
3	-1.92 (1.27)	-5.85 (0.40)	15.25	
4	2.29 (0.82)	-0.56 (0.23)	7.21	
5	-0.61 (0.97)	-1.93 (0.54)	2.49	
6	-0.43 (0.36)	-3.22 (0.94)	6.94	

Fold change was calculated by comparing expression in cells transfected with miR-146b-5p inhibitor to that in cells transfected with negative control, using the  $2^{-(\Delta\Delta Ct)}$  formula.

\* Statistical analysis was done using paired samples Student's *t*-test.

### STC1 is a target of miR-146b-5p in PTC

In order to identify the potential miR-146b-5p targets that might be involved in inhibition of the JNK/AP1 pathway, we tested the expression of the previously known miR-146b-5p targets that have JNK related functions, such as interleukin-1 receptor-associated kinase (IRAK1) and TNF receptor-associated factor 6 (TRAF6).<sup>15,21</sup> Screening of the expression of these targets in transfected thyroid cells by real time PCR revealed significant increased expression of IRAK1 (4.5 folds  $p=0.045$ ) but not of TRAF6 (1.9 fold,  $p=0.197$ ), after miR-146b-5p inhibition. Screening also revealed STC1 as one of the molecules with significant gene expression change after miR-146b-5p inhibition. A search by Target Scan program identified STC1 as one of the miR-146b-5p targets with seed location at position 2386-2393 of the STC1 3' untranslated region. We tested the expression of STC1 in thyroid tissues and cultured cells by quantitative real time PCR. Our results showed significant increase in the expression of SCT1 in thyroid cells transfected with miR-146b-5p inhibitor when compared to cells with negative control (Table 3). Our results also showed that STC1 mRNA expression in PTC cases with high miR-146b-5p level, is significantly down-regulated when compared to STC1 expression in tissues from MNG and NIFTP cases with low miR-146b-5p expression (Table 2). Expression of STC1 was also found to be significantly more downregulated in PTCs with negative p-JNK compared to PTCs with positive p-JNK ( $P=0.01$ ) (Figure 5c). To test if the expression of STC1 detected by PCR is due to STC1 expression by thyroid tumor cells specifically, we did immunostaining with STC1 specific antibody. Our preliminary qualitative results confirmed that STC1 protein is localized in the cytoplasm and nuclei of the thyroid follicular cells in MNG, NIFTP and some PTC cases (Figure 7).

### Discussion

MiR-146b-5p is associated with a complex network of gene regulation that could be tissue and stage-dependent, targeting different mRNA species in different situations. Many studies, including ours,<sup>23</sup> reported the upregulation of miR-146b-5p in thyroid cancer. However, few only reported on the signal transduction pathways regulated by miR-146b-5p and their functional impact in PTC development; These studies have demonstrated the role of miR-146b-5p in regulating NFκB, WNT, and TGFβ signaling pathways through targeting of

their adapter molecules, IRAK1, ZNRF3, and SMAD4, respectively.<sup>20–22</sup> In this work, we have demonstrated the role of miR-146b-5p in regulating the stress-activated protein kinase pathway and targeting STC1 which is not reported before.

The stress-activated protein kinase/c-Jun N-terminal kinase (SAPK/JNK) is a subfamily of the mitogen-activated protein kinase (MAPK) superfamily and has multiple functions in cancer ranging from cell proliferation to apoptosis depending on the stimuli and the cell type.<sup>36,37</sup> During carcinogenesis, many stress factors like oncogenic stress, oxidative stress, hypoxia, cytokines, etc., accumulate and activate the cellular stress responses. Upon activation by stress stimuli, JNK gets phosphorylated and is translocated to the nucleus where it phosphorylates c-jun. This leads to the formation of activator protein-1 (AP1), a transcription factor that up-regulates the expression of a wide variety of proteins involved in multiple cellular mechanisms.<sup>38</sup> Our transfection experiments showed that the relative luciferase activity of the JNK/AP1 pathway increased significantly after inhibition of miR-146b-5p in PTC samples with high miR-146b-5p endogenous level (Table 1). Inhibition of miR-146b-5p had only a minimal effect on the AP1 activity in other thyroid samples with low miR-146b-5p endogenous level, and on the activities of other pathways, which reflects the specific effect of miR-146b-5p on JNK/AP1 pathway. Measurement of the endogenous JNK/AP1 activity in thyroid cells also showed that its activity is inversely correlated with the expression of miR-146b-5p in PTC (Figure 2). Immunofluorescence and immunoblot experiments confirmed the increased activity of JNK/AP1 after miR-146b-5p inhibition in cultured PTC cells (Figures 3 and 4). Moreover, our results showed that the presence of active JNK is associated with lower miR-146b-5p expression in clinical tissue samples (Figure 5).

AP1 activity can be detected downstream of the mitogen-activated protein kinases (MAPKs), like ERK, JNK, or p38 pathways. Regulation of these pathways involves an immense network of enzymes, substrates, and regulatory mechanisms that are beyond the scope of this paper. The luciferase reporter assays did not show a significant effect of miR-146b-5p inhibition on the activity of other MAPK related transcription factors including ELK1, NFκB, and p53 (Table 1). Immunofluorescence staining of cultured PTC cells showed that ERK, p38, and NFκB activities are not affected by inhibition of miR-146b-5p (Figure S1). This can be due to the effect of cell culture environment affecting the pre-transfection pathways activity in a way masking the modulatory effect of miR-146b-5p. Another possibility can be the lack of proper stimuli to initiate the activity of these pathways, considering that miR-146b-5p might act as a promoter and not an initiator in the regulation of these pathways. Although we cannot definitely exclude an effect of miR-146b-5p on ERK and p38 pathways, the increase in AP1 activity after miR-146b-5p inhibition with no significant changes in other MAPK related transcription factors (Table 1, Figure S1) along with the expression pattern of p-JNK in cultured thyroid cells and PTC tissues, that appeared to be inversely correlated with miR-146b-5p expression (Figures 3, 4 and 5), indicate that miR-146b-5p has an inhibitory effect specific for the JNK/AP1 pathway.

Inhibition of AP1 pathway by miR-146b-5p has been implied in previous studies that investigated miRNA regulation

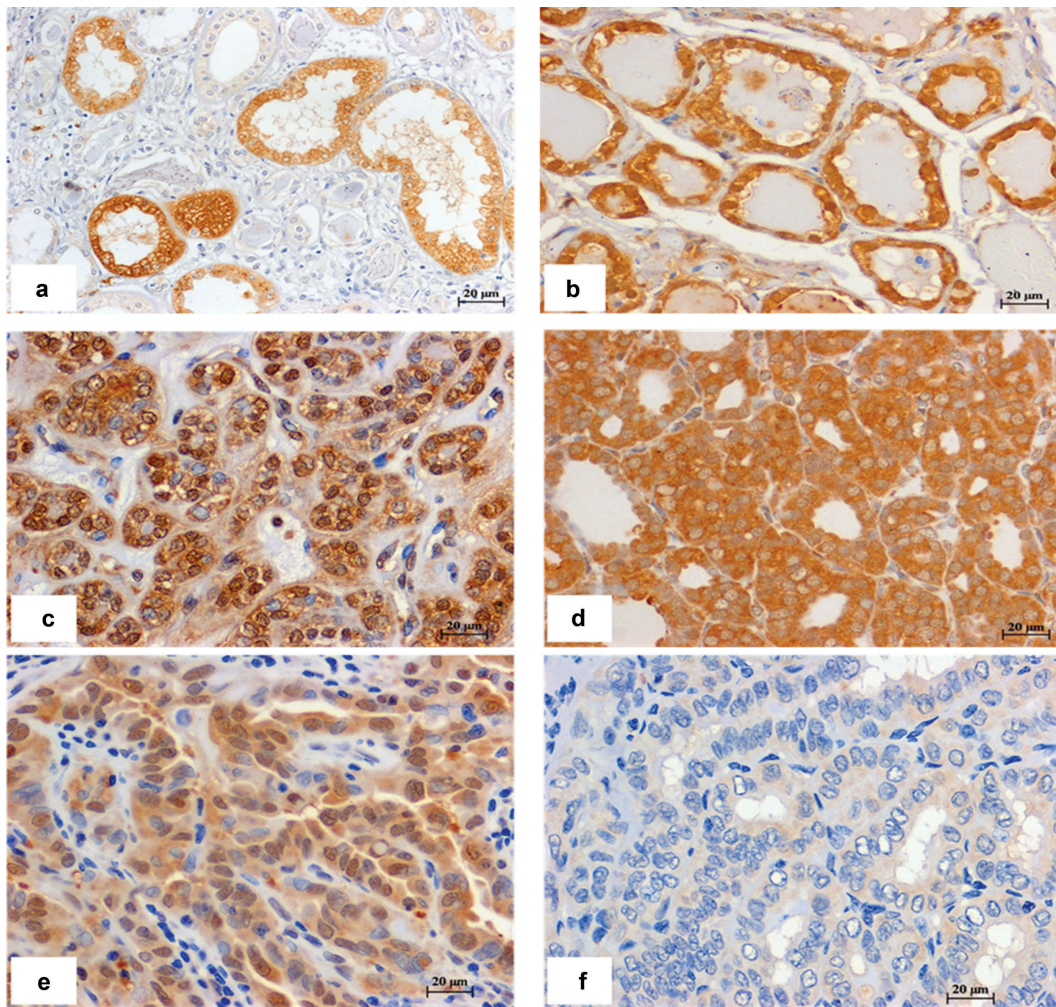


**Figure 7.** Immunohistochemistry stain of STC1 in different thyroid lesions. (a) Kidney tissue used as a positive control. (b) MNG, (c) NIFTP, (d, e) PTC, these cases express low level of miR-146b-5p and show positive STC1 staining in the cytoplasm/nucleus of thyroid follicular cells. (f) PTC sample with high miR-146b-5p expression showing negative staining of STC1. Scale bar is 20 µM.

of the immune response. These studies showed that in immune cells, miR-146a that has close mature sequence to miR-146b, targets IRAK1 and TRAF6, which potentially affect several signaling pathways including the NFκB, p42/p44 MAPK, and JNK/AP1 pathways.<sup>39,40</sup> These studies also suggested that miR-146b-5p expression is regulated by AP1 and up-regulation of miR-146b-5p following LPS stimulation could provide a negative feedback regulation to inhibit the NFκB signaling in macrophages and monocytes.<sup>40,41</sup> On the other hand, studies in LPS-treated human gingival fibroblasts (HGFs) could not find similar AP1 dependence. They reported that in HGFs, miR-146a/b expression was specifically dependent on NFκB but not ERK or JNK signaling.<sup>42</sup> In this study, we showed that miR-146b-5p affects the expression of IRAK1 but not that of TRAF6 (Results – Section 5). So although miR-146b-5p mediated down-regulation of JNK/AP1 pathway activity might be through targeting IRAK1, this possibility was reduced by the luciferase results which showed no effect of miR-146b-5p on the NFκB or ERK signaling activity (Table 1). Worth to note here, that in our transfection experiments we did not use any form of immune stimulation similar to the ones used in the above-mentioned studies. Inhibition of the JNK/AP1 pathway by miR-146b-5p that we are showing here is not a response to

in vitro immune stimuli but is an endogenous mechanism characterizing papillary thyroid cancer cells in culture and in patients' tissues, which is not reported before.

JNK/AP1 pathway is a key regulator of many cellular events, including cell death.<sup>36–43</sup> JNK/AP1 has pro- or anti-apoptotic functions, depending on cell type, nature of the death stimulus, duration of its activation and the activity of other signaling pathways. Studies have shown that in response to chronic stress, JNK/AP1 activates the apoptosis pathway in order to eliminate the stressed cells. Yet, it is debatable whether JNK is an intrinsic component of the apoptotic machinery or it only modulates apoptosis.<sup>37,44</sup> Recent studies have demonstrated that the JNK pathway is an important determinant of the Warburg effect in tumor cells and provides a mechanistic link between apoptosis and metabolism.<sup>45</sup> It was shown that inhibition of the JNK pathway promoted the Warburg effect in hepatocellular carcinoma while enhanced JNK phosphorylation inhibited the Warburg effect with consequential cell death.<sup>46</sup> Our results showed that miR-146b-5p has a negative regulatory effect on cell death in PTC cells upon exposure to oxidative stress (Figure 6). Inhibition of miR-146b-5p without exposure to stress had only a minimal effect on cell death (Figure 6), which agrees with previously published findings that activation of the JNK pathway is needed

to promote apoptosis but cannot initiate the apoptotic mechanisms.<sup>44–46</sup> We are suggesting here that cancer cells up-regulate miR-146b-5p to reduce the activity of the JNK/AP1 pathway in order to evade the carcinogenesis related stress induced cell death. A possibility can be that miR-146b-5p is up-regulated in PTC in response to the activation of JNK/AP1 pathway by stress stimuli during carcinogenesis, and then acts in a feedback mechanism to inhibit this pathway and promote survival.

Stanniocalcin-1 (STC1) is a molecule with multiple biological functions and with a 3'UTR site complementary to miR-146b-5p. Our results demonstrated that STC1 expression is upregulated in thyroid-cultured cells after miR-146b-5p inhibition (Table 3). Our results also showed that expression of STC1 in thyroid tissues has an inverse correlation with the expression of miR-146b-5p; STC1 mRNA and protein expression in PTC (high miR-146b-5p level) is significantly downregulated when compared to STC1 gene expression in MNG and NIFTP (low miR-146b-5p) (Table 2, Figure 7). These results prove that miR-146b-5p targets and regulates the expression of STC1 in thyroid tissues. A recent study reported multiple expression patterns of STC1 in thyroid tumor cell lines and thyroid tumor tissues that could not be explained or correlated with the types of cancer.<sup>35</sup> Regulation by miR-146b-5p can be the reason for the variable STC1 expression patterns observed in the above-mentioned study. Our preliminary results showing high expression of STC1 in benign cases and lower expression in PTC, suggest that STC1 functions against malignancy in thyroid cells. Further investigation of the expression and function of STC1 in thyroid cancer is needed.

STC1 has been reported previously to be associated with the activation of the JNK pathway. A recent study in breast cancer cells showed that phosphorylation of JNK and c-Jun was increased after STC-1 treatment but not the phosphorylation of ERK and p38.<sup>47</sup> Another study showed that STC1 enhances metastatic potential of hepatocellular carcinoma via JNK signaling.<sup>48</sup> Therefore, we can speculate that the inhibitory effect of miR-146b-5p on JNK activation can be mediated by, or at least associated with, the inhibition of STC1 expression in PTC cells. Moreover, it was shown that STC1 expression reduces cell survival under conditions of oxidative stress.<sup>32</sup> A recent study also reported that STC1 overexpression reduces energy metabolism in hepatocellular carcinoma leading to a reduction of tumor growth.<sup>49</sup> Reduced expression of STC1 and inhibition of JNK/AP1 pathway caused by miR-146b-5p up-regulation in PTC, possibly constitute a protective mechanism used by cancer cells to support cellular metabolism and resist death events in response to cellular stress. The intimate relation of miRNAs with the cellular stress pathways is revealed in many studies describing how stress signaling potentially alters the function of miRNAs and how miRNAs fine-tune the expression of components of the stress signaling cascades and modulate cellular adaptation to stress.<sup>50–54</sup> Since cellular stress is considered a vector of pathology in many chronic diseases including cancer, modulation of components of the stress response is a promising therapeutic avenue that can be attained through miRNA manipulation, and specifically through miR-146b-5p targeting.

## Conclusion

The impact of this study is at least two-fold: First, we showed that miR-146b-5p down-regulates the activation of JNK/AP1 pathway and protects PTC cells from cell death in response to oxidative stress. Second, we reported for the first time that STC1, an emerging stress and carcinogenesis-related molecule, is a miR-146b-5p target and its expression in thyroid cells is controlled by miR-146b-5p. The ability to modulate the JNK pathway and STC1 expression in cancer cells, advocates miR-146b-5p as one of the regulators of the stress-induced cell death and cellular metabolism which offer a novel therapeutic avenue in cancer management.

## Materials and methods

### Tissue samples

Formalin fixed paraffin embedded (FFPE) thyroid tissues were obtained from the archives of the histopathology unit at Kuwait Cancer Control hospital. All cases were microscopically reviewed by two consultant histopathologists (R.H. A. and N.A.B.) following the WHO classification of endocrine tumors published in 2017.<sup>55</sup> Groups were classified as follows: Classic PTC (cPTC) includes the conventional infiltrative PTC composed predominantly of papillae; NIFTP, the non-invasive follicular neoplasm with PTC nuclear features, classification was done according to the criteria set by the Endocrine Pathology Society<sup>56</sup> and adopted by the WHO.<sup>55</sup> The FFPE samples used in this study were 30 cPTC, 10 NIFTP, and 10 hyperplasia/multinodular goiter (MNG) cases (used as controls). Fresh thyroid tissues were also obtained and used for primary cell culture. These were portions of thyroid specimens, of partial or total thyroidectomy, that could be spared after the routine gross and histopathological procedures. Taking these specimens did not affect in any way the quality of the health care provided to the patients. We are presenting here the results from 16 cases: 13 PTCs and 3 cases of MNG used as controls. Ethical approval to conduct this study was obtained from the Kuwait Ministry of Health and from Kuwait University Health Sciences Center ethics committees. All methods were performed in accordance with the relevant guidelines and regulations approved by the ethics committee of Kuwait Ministry of Health.

### Primary thyroid cell culture

Thyroid tissues were transported in transport culture medium (HBSS solution enriched with 100 U/mL penicillin, 100 µg/mL streptomycin, and 2.5 µg/mL amphotericin) immediately to our laboratory. Tissues were digested by incubation in 20 ml of culture medium enriched with 1.25 mg/ml of Collagenase Type A and 10 mg/ml of Dispase II at 37°C for 90 min with the shaker set at around 80 rpm. Dissolved materials were filtered through a Thermo Scientific Piercer tissue strainer (Sigma) to remove undigested tissue fragments. Cells were collected by centrifugation for 5 min at 1200 g. The supernatant was poured back to the remaining tissue pieces and the procedure was

repeated several times, until all thyroid tissue was fully dissolved. Separated cells were cultured in culture flasks in complete F12 growth medium with 10% fetal calf serum at 37°C and 5% CO<sub>2</sub>. The cells were maintained to reach confluence and media were changed every 3–4 days. Cultured thyroid cells used to perform the functional tests were obtained from the first passage (within 1–2 weeks of culture) to avoid possible overgrowth by fibroblasts. Cells were characterized by immunostaining with cytokeratin specific antibody to confirm that they are epithelial cells and with thyroglobulin specific antibody to confirm that they are thyroid follicular cells (Figure 1).

### **Labeling and transfection of miR-146b-5p inhibitor**

The miScript miR-146b-5p Inhibitor (Qiagen) was labelled with fluorescent dye using the Silencer® fluorescein (FAM™ dye) RNA Labeling Kit (Thermo Fisher- AM1634) following the manufacture instructions. A mixture containing; 22.5 µL Nuclease-free Water, 5 µL 10X Labeling Buffer, 15 µL siRNA at 50 µM and 7.5 µL of FAM™ Labeling Reagent was prepared and incubated for 1 hr at 37°C in the dark. The labeled siRNA was precipitated by addition of 5 µL of 5M NaCl, 125 µL cold 100% ethanol and chilling for 30 min at – 20°C. Finally, the precipitant was pelleted by centrifugation at ≥8,000 x g for 15 min and washed with 175 µL of 70% ethanol. Cultured cells, at a density of  $1 \times 10^6$  cells, were transfected using 15 µL of HiPerFect Transfection Reagent (Qiagen) and 150 ng of miScript miR-146b-5p Inhibitor (Qiagen) or a negative control (Qiagen). In all transfection experiments endogenous miR-146b-5p levels were quantified by real-time PCR before and after transfection to ensure that transfection of miScript miR-146b-5p inhibitor strongly reduced the amount of detectable endogenous miR-146b-5p.

### **Luciferase reporter assay**

The effect of miR-146b-5p on signaling pathways essential for carcinogenesis was tested using the Signal Finder Cancer Pathway Reporter Array (Qiagen). These reporter assays are based on dual-luciferase technology. Each reporter consists of a mixture of a pathway-focused transcription factor-responsive firefly luciferase construct and a constitutively expressing Renilla luciferase construct. The pathways tested here were: MAPK/JNK, MAPK/ERK, NFκB, Hypoxia and p53 with the corresponding transcription factors reporters, AP1, ELK1/SRF, NFκB, HIF1A and p53 respectively. Cultured cells were plated at a density of  $8 \times 10^4$  cells/well in antibiotic free minimal essential media in 96 well plate containing the transcription factor-responsive reporters, negative control, and positive control constructs. 1.5 µL HiPerFect Transfection Reagent (Qiagen) were added to all wells (8 wells for each pathway); 15 ng of hsa-miR-146b-5p miScript miRNA Inhibitor (Qiagen) were added in 4 wells and the other 4 wells were kept without the inhibitor to be used as negative controls. After 48 hours of incubation, the firefly luciferase activity was stopped by adding 100µL of Dual-Glo® Stop & Glo® Reagent (Promega). 100µL of the Dual-Glo® Luciferase Reagent (Promega) containing buffer and substrate were added and the luminescence was measured by Thermo

Scientific Appliskan Plate Reader. Firefly/Renilla activity ratios were generated for experimental (with miR-146b-5p inhibitor) and control (negative control) transfections. The change in the activity of each signaling pathway is determined by comparing the normalized luciferase activities of the reporter in experimental versus control transfectants using the formula, Fold Change = (firefly/renilla ratio of experimental sample)/(firefly/renilla ratio of control sample). All transfections were performed in quadruplicate for each of the reporter assays. Transfection efficiency was estimated by observing GFP expression (a constitutively expressing GFP construct containing Monster Green® Fluorescent Protein) in the positive control wells by fluorescence microscopy.

### **Reverse transcription and quantitative real-time PCR amplification**

Total RNA from cultured cells and from paraffin-embedded thyroid tissues was isolated using TRIzol (Ambion) and miRNeasy FFPE Kit (Qiagen, Hilden, Germany) respectively, following the manufacturers' instructions. The yield and quality of the RNA samples were determined by spectrophotometry using 260/280 ratios. Reverse transcription of cDNA was done using 100 ng of the extracted total RNA and the miScript II RT Kit (Qiagen) according to the manufacturer's instructions. cDNA was mixed with RT<sup>2</sup> SYBR Green Mastermix (Qiagen), and RT<sup>2</sup> qPCR Primer Assay specific primers (STC1 or miR-146b-5p specific) (Qiagen), and amplification reactions were set in 96-well plates. HPRT was used as housekeeping gene and PCR reactions were run on an ABI 7500 Fast Block real-time PCR machine. All samples including the house keeping genes were run in triplicates and mean CT value with standard deviation were calculated for each sample. Expression is calculated using the relative quantification method ( $\Delta\text{Ct} = \text{CT of target normalized to CT of house-keeping genes}$ ). Expression in the test groups are compared to control group using the formula ( $\Delta\Delta\text{CT} = \Delta\text{CT of test group} - \Delta\text{CT of control group}$ ), and results are finally presented as fold change ( $2^{-\Delta\Delta\text{CT}}$ ).<sup>57</sup>

### **Immunofluorescence and immunohistochemistry stain**

Expression and subcellular localization of AP1 and of phosphorylated JNK (p-JNK) were tested by indirect immunofluorescence staining and confocal microscopy. Expression of STC1 was assessed by immunohistochemistry. Staining was done on FFPE tissue sections or cultured cells grown in slide dishes and fixed with cold methanol. The antibodies used were anti-phospho-JNK (Cell signaling), anti-AP1 (Sigma), and anti-STC1 (Santa Cruz). Primary antibodies were diluted according to manufacturers' recommendations and incubated at 4°C overnight. Secondary antibodies labeled with Alexa Fluor 555 and Alexa Fluor 488 (Invitrogen) or HRP (Dako), were incubated for one hour at room temperature. For FFPE tissue sections the nonspecific background was blocked using blocking solution (Dako) and the staining was assessed qualitatively and scored as positive or negative. Positive score is given only when more than 10% of tumor cells show non-ambiguous staining. Staining of immune cells

or any infiltrating cells other than the tumor follicular cells with the anti-p-JNK or anti-STC1 antibodies was not considered as positivity.

### Immunoblotting

20 µg of protein was mixed with loading buffer and rainbow marker (14,300–220,000 Da, Amersham Pharmacia Biotech Ltd., U.K.). Electrophoresis was performed using SDS-PAGE gel (SDS PAGE; 5–14% polyacrylamide gradient gels). Protein was transferred to PVDF membranes at a stable current of 300 mA overnight at 4°C. The efficiency of transfer was confirmed by staining the gel with Coomassie blue stain. Blocking was done for 1 h at room temperature with 10% non-fat dry milk in TBS-T. The primary antibody diluted in non-fat dry milk in TBS-T was incubated overnight at 4°C. Membranes were incubated with the secondary antibody overnight at room temperature then washed several times. Protein bands were detected by chemiluminescence using ECL-Plus kit (Amersham Pharmacia Biotech Ltd.).

### Apoptosis assay

Cultured cells were harvested by trypsinization, centrifuged and washed with cold PBS. The cells were resuspended in 400 µl of binding buffer (Invitrogen). 2 µl of both Annexin V and Propidium iodide was added and the cells were incubated on ice for 20 min. The stained cells were analyzed by flow cytometry. Oxidative stress was induced by treating the cancer cells with Paraquat (3 µM) for 24 h before staining and flow cytometry analysis.

### Statistical analysis

The expression level of miR-146b-5p and STC1 gene in PTC, NIFTP, and MNG groups were compared using student's *t*-test. The difference in gene expression level and cell signaling activity between matched samples (transfected with miR-146b-5p inhibitor versus controls) was determined using paired-sample Student's *t*-test. In all tests, significance was considered with a *p*-value of <0.05.

### Acknowledgments

We acknowledge the technical assistance of Mrs. Jeena Prashanth and Mr. Mohammed Reza, and the research core facility of the health sciences center, Kuwait University, project # SRUL 02/13.

### Funding

This work is funded by Kuwait University, Research Sector, research grants # MG 02/13 and # MY 08/15; And by Kuwait Foundation for the Advancement of Sciences [P11563MM02]

### Authors contributions

A.A. did the study design, data analysis and manuscript writing. I.J. did the molecular and functional experiments and data analysis. H.M. did the immunostaining experiments and contributed to tissue culture and confocal microscopy. R.A. and N.A. did the sample collection and

histopathological classification. O.M. contributed to overall coordination and funding.

### Ethical approval

Ethical approval to conduct this study was obtained from Kuwait Ministry of Health and from Kuwait University Health Sciences Center ethics committee. All methods were performed in accordance with the relevant guidelines and regulations approved by the ethics committee of Kuwait Ministry of Health.

### Conflict of interest

None of the authors have any conflict of interest in this manuscript.

### Data availability

The datasets generated during and/or analyzed during the current study are available from the corresponding author on reasonable request.

### ORCID

Abeer Al-Abdallah  <http://orcid.org/0000-0001-8577-802X>

### References

1. Lim H, Devesa SS, Sosa JA, Check D, Kitahara CM. Trends in thyroid cancer incidence and mortality in the United States, 1974–2013. *JAMA*. 2017;317(13):1338–1348. doi:10.1001/jama.2017.2719.
2. Davies L, Welch HG. Current thyroid cancer trends in the United States. *JAMA Otolaryngol Head Neck Surg*. 2014;140:317–322. doi:10.1001/jamaoto.2014.1.
3. Riesco-Eizaguirre G, Santisteban P. Advances in the molecular pathogenesis of thyroid cancer: lessons from the cancer genome. *Eur J Endocrinol*. 2016;175(5):R203–17. doi:10.1530/EJE-16-0202.
4. Vuong HG, Altibi AM, Abdelhamid AH, Ngoc PU, Quan VD, Tantawi MY, Elfil M, Vu TL, Elgebaly A, Oishi N, et al. The changing characteristics and molecular profiles of papillary thyroid carcinoma over time: a systematic review. *Oncotarget*. 2017;8(6):10637–10649. doi:10.18632/oncotarget.v8i6.
5. Lee MY, Ku BM, Kim HS, Lee JY, Lim SH, Sun JM, Lee SH, Park K, Oh YL, Hong M, et al. Genetic alterations and their clinical implications in high-recurrence risk papillary thyroid cancer. *Cancer Res Treat*. 2017;49(4):906–914. doi:10.4143/crt.2016.424.
6. Calin GA, Croce CM. MicroRNA signatures in human cancers. *Nat Rev Cancer*. 2006;6(11):857–866. doi:10.1038/nrc1997.
7. Lu J, Getz G, Miska EA, Alvarez-Saavedra E, Lamb J, Peck D, Sweet-Cordero A, Ebert BL, Mak RH, Ferrando AA, et al. MicroRNA expression profiles classify human cancers. *Nature*. 2005;435(7043):834–838. doi:10.1038/nature03702.
8. Palanichamy JK, Rao DS. miRNA dysregulation in cancer: towards a mechanistic understanding. *Front Genet*. 2014;18(5):54.
9. Detassis S, Grasso M, Del Vescovo V, Denti MA. microRNAs make the call in cancer personalized medicine. *Front Cell Dev Biol*. 2017;22(5):86. doi:10.3389/fcell.2017.00086.
10. Stokowy T, Gawel D, Wojtas B. Differences in miRNA and mRNA profile of papillary thyroid cancer variants. *Int J Endocrinol*. 2016;2016:1427042. doi:10.1155/2016/1427042.
11. Tang J, Kong D, Cui Q, Wang K, Zhang D, Yuan Q, Liao X, Gong Y, Wu G. Bioinformatic analysis and identification of potential prognostic microRNAs and mRNAs in thyroid cancer. *PeerJ*. 2018;4(6):e4674. doi:10.7717/peerj.4674.
12. Chapelle AD, Jazdzewski K. MicroRNAs in Thyroid Cancer. *J Clin Endocrinol Metab*. 2011;96(11):3326–3336. doi:10.1210/jc.2011-1004.

13. Chou CK, Liu RT, Kang HY. MicroRNA-146b: A novel biomarker and therapeutic target for human papillary thyroid cancer. *Int J Mol Sci.* 2017 15;18(3):E636. doi:10.3390/ijms18030636.
14. Li Y, Zhang H, Dong Y, Fan Y, Li Y, Zhao C, Wang C, Liu J, Li X, Dong M, et al. MiR-146b-5p functions as a suppressor miRNA and prognosis predictor in non-small cell lung cancer. *J Cancer.* 2017 30;8(9):1704–1716. doi:10.7150/jca.16961.
15. Liu J, Xu J, Li H, Sun C, Yu L, Li Y, Shi C, Zhou X, Bian X, Ping Y, et al. miR-146b-5p functions as a tumor suppressor by targeting TRAF6 and predicts the prognosis of human gliomas. *Oncotarget.* 2015;6(30):29129–29142. doi:10.18632/oncotarget.4895.
16. Ramírez-Moya J, Wert-Lamas L, Santisteban P. MicroRNA-146b promotes PI3K/AKT pathway hyperactivation and thyroid cancer progression by targeting PTEN. *Oncogene.* 2018;37:3369–3383. doi:10.1038/s41388-017-0088-9.
17. Chou CK, Chen RF, Chou FF, Chang HW, Chen YJ, Lee YF, Yang KD, Cheng JT, Huang CC, Liu RT. MiR-146b is highly expressed in adult papillary thyroid carcinomas with high risk features including extrathyroidal invasion and the brafv600e mutation. *Thyroid.* 2010;20:489–494. doi:10.1089/thy.2009.0027.
18. Lima CR, Geraldo MV, Fujiwara CS, Kimura ET, Santos MF. MiRNA-146b-5p upregulates migration and invasion of different papillary thyroid carcinoma cells. *BMC Cancer.* 2016;16(16):108. doi:10.1186/s12885-016-2146-z.
19. Chou CK, Yang KD, Chou FF, Huang CC, Lan YW, Lee YF, Kang HY, Liu RT. Prognostic Implications of miR-146b expression and its functional role in papillary thyroid carcinoma. *J Clin Endocrinol Metab.* 2013;98:E196–205. doi:10.1210/jc.2012-2666.
20. Deng X, Wu B, Xiao K, Kang J, Xie J, Zhang X, Fan Y. MiR-146b-5p promotes metastasis and induces epithelial-mesenchymal transition in thyroid cancer by targeting ZNF3. *Cell Physiol Biochem.* 2015;35:71–82. DOI:10.1111/j.1365-2141.1975.tb00536.x.
21. Chou CK, Chi SY, Huang CH, Chou FF, Huang CC, Liu RT, Kang HY. IRAK1, a target of miR-146b, reduces cell aggressiveness of human papillary thyroid carcinoma. *J Clin Endocrinol Metab.* 2016;101:4357–4366. doi:10.1210/jc.2016-2276.
22. Geraldo MV, Yamashita AS, Kimura ET. MicroRNA miR-146b-5p regulates signal transduction of TGF- $\beta$  by repressing SMAD4 in thyroid cancer. *Oncogene.* 2012 12;31(15):1910–1922. doi:10.1038/ncr.2011.381.
23. Jahanbani I, Al-Abdallah A, Ali RH, Al-Brahim N, Mojiminiyi O. Discriminatory miRNAs for the management of papillary thyroid carcinoma and noninvasive follicular thyroid neoplasms with papillary-like nuclear features. *Thyroid.* 2018;28(3):319–327. doi:10.1089/thy.2017.0127.
24. Madsen KL, Tavernini MM, Yachimec C, Mendrick DL, Alfonso PJ, Buerger M, Olsen HS, Antonaccio MJ, Thomson AB, Fedorak RN. Stanniocalcin: a novel protein regulating calcium and phosphate transport across mammalian intestine. *Am J Physiol.* 1998;274(1 Pt 1):G96–102. doi:10.1152/ajpgi.1998.274.1.G96.
25. Olsen HS, Cepeda MA, Zhang QQ, Rosen CA, Vozzolo BL, Wagner GF. Human stanniocalcin: a possible hormonal regulator of mineral metabolism. *Proc Natl Acad Sci USA.* 1996;93:1792–1796. doi:10.1073/pnas.93.5.1792.
26. Kahn J, Mehraban F, Ingle G, Xin X, Bryant JE, Vehar G, Schoenfeld J, Grimaldi CJ, Peale F, Draksharapu A, et al. Gene expression profiling in an in vitro model of angiogenesis. *Am J Pathol.* 2000;156:1887–1900. doi:10.1016/S0002-9440(10)65062-6.
27. Kanellis J, Bick R, Garcia G, Truong L, Tsao CC, Hemadmoghadam D, Poindexter B, Feng L, Johnson RJ, Sheikh-Hamad D. Stanniocalcin-1, an inhibitor of macrophage chemotaxis and chemokinesis. *Am J Physiol Renal Physiol.* 2003;286:F356–F362. doi:10.1152/ajprenal.00138.2003.
28. McCudden CR, James KA, Hasilo C, Wagner GF. Characterization of mammalian stanniocalcin receptors: mitochondrial targeting of ligand and receptor for regulation of cellular metabolism. *J Biol Chem.* 2002;277:45249–45258. doi:10.1074/jbc.M205954200.
29. Chang ACM, Jellinek DA, Reddel RR. Mammalian stanniocalcins and cancer. *Endocr Relat Cancer.* 2003;10:359–373. doi:10.1677/erc.0.0100359.
30. Fujiwara Y, Sugita Y, Nakamori S, Miyamoto A, Shiozaki K, Nagano H, Sakon M, Monden M. Assessment of stanniocalcin-1 mRNA as a molecular marker for micrometastases of various human cancers. *Int J Oncol.* 2000;16:799–804. doi:10.3892/ijo.16.4.799.
31. Lal A, Peters H, St Croix B, Haroon ZA, Dewhirst MW, Strausberg RL, Kaanders JH, van der Kogel AJ, Riggins GJ. Transcriptional response to hypoxia in human tumors. *J Natl Cancer Inst.* 2001;93:1337–1343. doi:10.1093/jnci/93.17.1337.
32. Nguyen A, Chang AC, Reddel RR. Stanniocalcin-1 acts in a negative feedback loop in the prosurvival ERK1/2 signaling pathway during oxidative stress. *Oncogene.* 2009;28:1982–1992. doi:10.1038/ncr.2009.65.
33. Welcsh PL, Lee MK, Gonzalez-Hernandez RM, Black DJ, Mahadevappa M, Swisher EM, Warrington JA, King MC. BRCA1 transcriptionally regulates genes involved in breast tumorigenesis. *Proc Natl Acad Sci USA.* 2002;99:7560–7565. doi:10.1073/pnas.062181799.
34. Lai KP, Law AY, Yeung HY, Lee LS, Wagner GF, Wong CK. Induction of stanniocalcin-1 expression in apoptotic human nasopharyngeal cancer cells by p53. *Biochem Biophys Res Commun.* 2007;356:968–975. doi:10.1016/j.bbrc.2007.03.074.
35. Hayase S, Sasaki Y, Matsubara T, Seo D, Miyakoshi M, Murata T, Ozaki T, Kakudo K, Kumamoto K, Ylaja K, et al. Expression of Stanniocalcin 1 in thyroid side population cells and thyroid cancer cells. *Thyroid.* 2015;25(4):425–436. doi:10.1089/thy.2014.0464.
36. Zeke A, Misheva M, Reményi A, Bogoyevitch MA. JNK signaling: regulation and functions based on complex protein-protein partnerships. *MMBR.* 2016;8(3):793–835.
37. Tournier C, Hess P, Yang DD, Xu J, Turner TK, Nimnual A, Bar-Sagi D, Jones SN, Flavell RA, Davis RJ. Requirement of JNK for stress-induced activation of the cytochrome c-mediated death pathway. *Science.* 2000 5;288(5467):870–874. doi:10.1126/science.288.5467.870.
38. Mendelson KG, Contois LR, Tevosian SG, Davis RJ, Paulson KE. Independent regulation of JNK p38 mitogen-activated protein kinases by metabolic oxidative stress in the liver. *Proc Natl Acad Sci USA.* 1996 12;93(23):12908–12913. doi:10.1073/pnas.93.23.12908.
39. Zhou R, O'Hara SP, Chen XM. MicroRNA regulation of innate immune responses in epithelial cells. *Cell Mol Immunol.* 2011;8(5):371–379. doi:10.1038/cmi.2011.19.
40. Taganov KD, Boldin MP, Chang KJ, Baltimore D. NF- $\kappa$ B-dependent induction of microRNA miR-146, an inhibitor targeted to signaling proteins of innate immune responses. *Proc Natl Acad Sci USA.* 2006 15;103(33):12481–12486. doi:10.1073/pnas.0605298103.
41. Hou J, Wang P, Lin L, Liu X, Ma F, An H, Wang Z, Cao X. MicroRNA-146a feedback inhibits RIG-1-dependent type I IFN production in macrophages by targeting TRAF6, IRAK1, and IRAK2. *J Immunol.* 2009;183:2150–2158. doi:10.4049/jimmunol.0900707.
42. Xie YF, Shu R, Jiang SY, Song ZC, Guo QM, Dong JC, Lin ZK. miRNA-146 negatively regulates the production of pro-inflammatory cytokines via NF- $\kappa$ B signalling in human gingival fibroblasts. *J Inflamm (Lond).* 2014 6;11(1):38. doi:10.1186/s12950-014-0038-z.
43. Dhanasekaran DN, Reddy EP. JNK-signaling: A multiplexing hub in programmed cell death. *Genes Cancer.* 2017;8(9–10):682–694. doi:10.18632/genesandcancer.155.
44. Liu J, Lin A. Role of JNK activation in apoptosis: A double-edged sword. *Cell Res.* 2005;15(1):36–42. doi:10.1038/sj.cr.7290262.
45. Papa S, Bubici C. Linking apoptosis to cancer metabolism: another missing piece of JuNK. *Mol Cell Oncol.* 2016;3:e1103398. doi:10.1080/23723556.2015.1103398.
46. Iansante V, Choy PM, Fung SW, Liu Y, Chai JG, Dyson J, Del Rio A, D'Santos C, Williams R, Chokshi S, et al. PARP14 promotes the Warburg effect in hepatocellular carcinoma by inhibiting JNK1-dependent PKM2 phosphorylation and activation. *Nat Commun.* 2015;6:7882. doi:10.1038/ncomms8882.
47. Han J, Jeon M, Shin I, Kim S. Elevated STC-1 augments the invasiveness of triple-negative breast cancer cells through

- activation of the JNK/c-Jun signaling pathway. *Oncol Rep.* **2016**;36(3):1764–1771. doi:[10.3892/or.2016.4977](https://doi.org/10.3892/or.2016.4977).
48. Chan KK, Leung CO, Wong CC, Ho DW, Chok KS, Lai CL, Ng IO, Lo RC, Stanniocalcin S. 1 promotes metastasis of hepatocellular carcinoma through activation of JNK signaling pathway. *Cancer Lett.* **2017**;10(403):330–338. doi:[10.1016/j.canlet.2017.06.034](https://doi.org/10.1016/j.canlet.2017.06.034).
  49. Leung C, Wong C. Effects of STC1 overexpression on tumorigenicity and metabolism of hepatocellular carcinoma. *Oncotarget.* **2018**;9(6):6852–6861. doi:[10.18632/oncotarget.v9i6](https://doi.org/10.18632/oncotarget.v9i6).
  50. Mendell JT, Olson EN. MicroRNAs in stress signaling and human disease. *Cell.* **2012**;148:1172–1187. doi:[10.1016/j.cell.2012.02.005](https://doi.org/10.1016/j.cell.2012.02.005).
  51. Byrd AE, Brewer JW. Micro(RNA) managing endoplasmic reticulum stress. *IUBMB Life.* **2013**;65(5):373–381. doi:[10.1002/iub.v65.5](https://doi.org/10.1002/iub.v65.5).
  52. Leung AK, Sharp PA. MicroRNA functions in stress responses. *Mol Cell.* **2010**;40(2):205–215. doi:[10.1016/j.molcel.2010.09.027](https://doi.org/10.1016/j.molcel.2010.09.027).
  53. Maurel M, Chevet E. Endoplasmic reticulum stress signaling: the microRNA connection. *Am J Physiol Cell Physiol.* **2013**;304:C1117–C1126. doi:[10.1152/ajpcell.00061.2013](https://doi.org/10.1152/ajpcell.00061.2013).
  54. Emde A, Hornstein E. miRNAs at the interface of cellular stress and disease. *Embo J.* **2014** 1;33(13):1428–1437. doi:[10.15252/embj.201488142](https://doi.org/10.15252/embj.201488142).
  55. Lam AK. Pathology of endocrine tumors update: World Health Organization new classification 2017—other thyroid tumors. *AJSP Rev Rep.* **2017**;22(4):209–216.
  56. Nikiforov YE, Seethala RR, Tallini G, Baloch ZW, Basolo F, Thompson LD, Barletta JA, Wenig BM, Al Ghuzlan A, Kakudo K, et al. Nomenclature revision for encapsulated follicular variant of papillary thyroid carcinoma. *JAMA Oncol.* **2016**;2:1023–1029. doi:[10.1001/jamaoncol.2016.0386](https://doi.org/10.1001/jamaoncol.2016.0386).
  57. Schmittgen TD, Livak KJ. Analyzing real-time PCR data by the comparative C(T) method. *Nat Protoc.* **2008**;3:1101–1108. doi:[10.1038/nprot.2008.73](https://doi.org/10.1038/nprot.2008.73).